



Numerical simulation of the land subsidence induced by groundwater mining

Hong Chen¹ · Yiguo Xue^{1,2} · Daohong Qiu¹

Received: 31 May 2022 / Revised: 21 September 2022 / Accepted: 26 September 2022 / Published online: 12 October 2022
© The Author(s), under exclusive licence to Springer Science+Business Media, LLC, part of Springer Nature 2022

Abstract

Land subsidence has become a widespread engineering geological problem, which can quickly induce many derived disasters. Over-exploitation of groundwater is one of the main factors of urban land subsidence. There is severe land subsidence in Jining, mainly induced by groundwater over-extraction. Therefore, the numerical simulation method is used in this paper to analyze and predict the law of land subsidence in Jining. Combined with the engineering geological and hydrogeological conditions of Jining City, a three-dimensional fluid–solid coupling model of land subsidence was established by using COMSOL software. The numerical results were verified using site monitoring data. The article predicts the land subsidence in the study area in 2030. In 2030, the maximum land subsidence is 224 mm. And this paper analyzes the land subsidence pattern under different groundwater extraction amounts. The results show that the land subsidence in the study area is effectively alleviated under the condition of reducing water extraction by 30%. It provides a basis for preventing and controlling land subsidence in Jining city. It is proved that land subsidence caused by groundwater extraction positively correlates with the pumping time and amount of water pumped.

Keywords Three-dimensional fluid–solid coupled model · Land subsidence · Groundwater pumping · Numerical simulation · Prediction

1 Introduction

Land subsidence is a slow-varying engineering geological problem in which loose underground rock and soil layers consolidate and compress under the action of natural factors or human activities, resulting in a reduction of ground elevation in a certain area [1, 2]. There are many triggering factors for ground subsidence, such as excessive exploitation of mineral resources such as oil and coal mines and groundwater [3–6].

Groundwater extraction is increasing due to the high use of water resources for industrial, agricultural, and other

activities. Over-exploitation of groundwater has become one of the most critical factors of land subsidence. More than 200 cities and regions worldwide have severe land subsidence due to the over-exploitation of groundwater [7]. Land subsidence has been observed in central and south-central Arizona in the United States, Mexico City, Bandung in Indonesia, Jakarta, and Bangkok in Thailand [8–11]. Many Chinese cities are also facing land subsidence problems. There are three significant areas of land subsidence in China: The Yangtze River Delta region, represented by Shanghai and Suzhou [12, 13]; The North China Plain, represented by Beijing and Tianjin [14, 15]; Fenwei Basin region, represented by Xi'an and Taiyuan [16, 17]. Urban ground subsidence caused by groundwater overdrafts has seriously affected infrastructure development and constrained sustainable economic development. This has had a severe negative impact on the development of the city.

Land subsidence caused by groundwater extraction has become a global problem. With the increasing demand for groundwater, land subsidence has been monitored and researched worldwide [18–20]. Research tools for land

Hong Chen and Yiguo Xue have contributed equally to this work.

✉ Yiguo Xue
xieagle@sdu.edu.cn

¹ Geotechnical and Structural Engineering Research Center, Shandong University, Jinan 250061, China

² School of Engineering and Technology, China University of Geosciences (Beijing), Beijing 100083, China

subsidence mainly include land subsidence mechanism research [21, 22], numerical simulation [23, 24] and intelligent monitoring methods [25, 26]. Numerical simulation can effectively predict urban land subsidence patterns [27–30]. To calculate the land subsidence in the Su-Xi-Chang region and Shanghai, Shi et al. [31] established a coupled water flow-settlement model consisting of a three-dimensional water flow model with variable coefficients and a one-dimensional settlement model. Tianjin Binhai New Area is one of the most serious areas of ground subsidence. Hu et al. [32] predicted the land subsidence of Tianjin Binhai New Area from 2011 to 2020 by establishing a numerical model. This provides a scientific basis for the sustainable development planning of the area. Giao et al. [33] developed quasi-3D modeling to analyze the role of artificial recharge in land subsidence control in Bangkok City. Larson et al. [34] developed an integrated numerical model of groundwater and land subsidence for the land subsidence problem in the Los Banos-Kettleman City area. This article analyzes the land subsidence pattern under the current pumping capacity and determines the optimal pumping capacity for the area. A numerical simulation is an effective tool for studying the land subsidence changes caused by groundwater over-extraction.

Land subsidence has become a common engineering geological problem, which can easily induce many secondary disasters. Jining is facing severe land subsidence, which has seriously affected the city's development. At present, there are few pieces of research on land subsidence in Jining. Therefore, this paper uses numerical simulation to study the land subsidence in Jining.

According to the engineering geological and hydrogeological data of the Jining urban area, the fluid–structure coupling model of land subsidence is established by COMSOL software. The model reenacts historical changes in land subsidence in the Jining study area and predicts land subsidence change patterns to 2030. This paper establishes the land subsidence model under different extraction amounts. And the land subsidence law under 30% increase and 30% decrease of pumping volume is analyzed. This paper proposes engineering measures to control land subsidence, laying the foundation for preventing and controlling land subsidence in the Jining demonstration area.

The rest of the paper is organized as follows: Sect. 2 describes the geological and hydrological conditions of the study area. Section 3 introduces the theoretical basis and the establishment of the numerical model and verifies the numerical model. In Sect. 4, the numerical results are compared and analyzed. Section 5 is the conclusion of this paper.

2 Geological and hydrogeological conditions

Jining City is located in the southwestern part of Shandong Province, combining four provinces: Jiangsu, Shandong, Henan, and Anhui. Jining city planning area extended by 2.5 km as the scope of the survey area. The area of this study is about 207km², which is the primary groundwater exploitation area in the urban area of Jining.

The study area is a warm-temperate semi-humid monsoon climate zone with four distinct seasons during the year. The interannual climate is characterized by spring droughts, summer floods, and late autumn droughts. The multi-year average precipitation from 1980 to 2019 is 668.1 mm, with an average annual maximum of 1088.67 mm and an average annual minimum of 397.72 mm. The main rivers in the district are Guangfuhe and Beijing-Hangzhou Canal, which flow through the district from north to south and are injected into Nanyanghu. These belong to the Nansihu water system in the Huaihe River Basin.

The groundwater-bearing rock group in the area is the loose rock type pore water-bearing rock group, followed by the Carbonate fractured karst water-bearing rock group (Fig. 1a). Loose rock type pore water-bearing rock group is stored in the alluvial and alluvial sand layers of the new tertiary-quaternary loose rock formation. The aquifer mainly consists of coarse sand, medium sand, and fine sand. The carbonate fractured karst water-bearing rock group consists of Cambrian-Ordovician carbonate rocks. Affected by geological structure and stratum lithology, the development of fissure karst is not uniform, and the water-richness varies greatly.

The survey area is flat and open, with various landforms such as low hills, plain depressions, and lakeside depressions. The regional stratigraphy belongs to the North China stratigraphic region. The stratigraphic age from old to new mainly includes Paleozoic Ordovician, Carboniferous-Permian, Mesozoic Jurassic, and Cenozoic Quaternary (Fig. 1b).

The thickness of the Neoproterozoic-Quaternary loose layer in Jining City reaches 220–300 m, and the lithology is the alternate accumulation of clayey soil and sandy soil. The topsoil layer is a loose clayey layer of the Quaternary Holocene, with a thickness of 2–10 m. It is underlain by an alternating accumulation of clay, sand, and gravel layers of the Pleistocene Quaternary, during which 4–7 layers of water-bearing sands have developed. The water-bearing sand layer is vertically concentrated in two relatively enriched sand layers below 10–40 m and 60 m burial depth. They constitute two aquifer groups: shallow pore

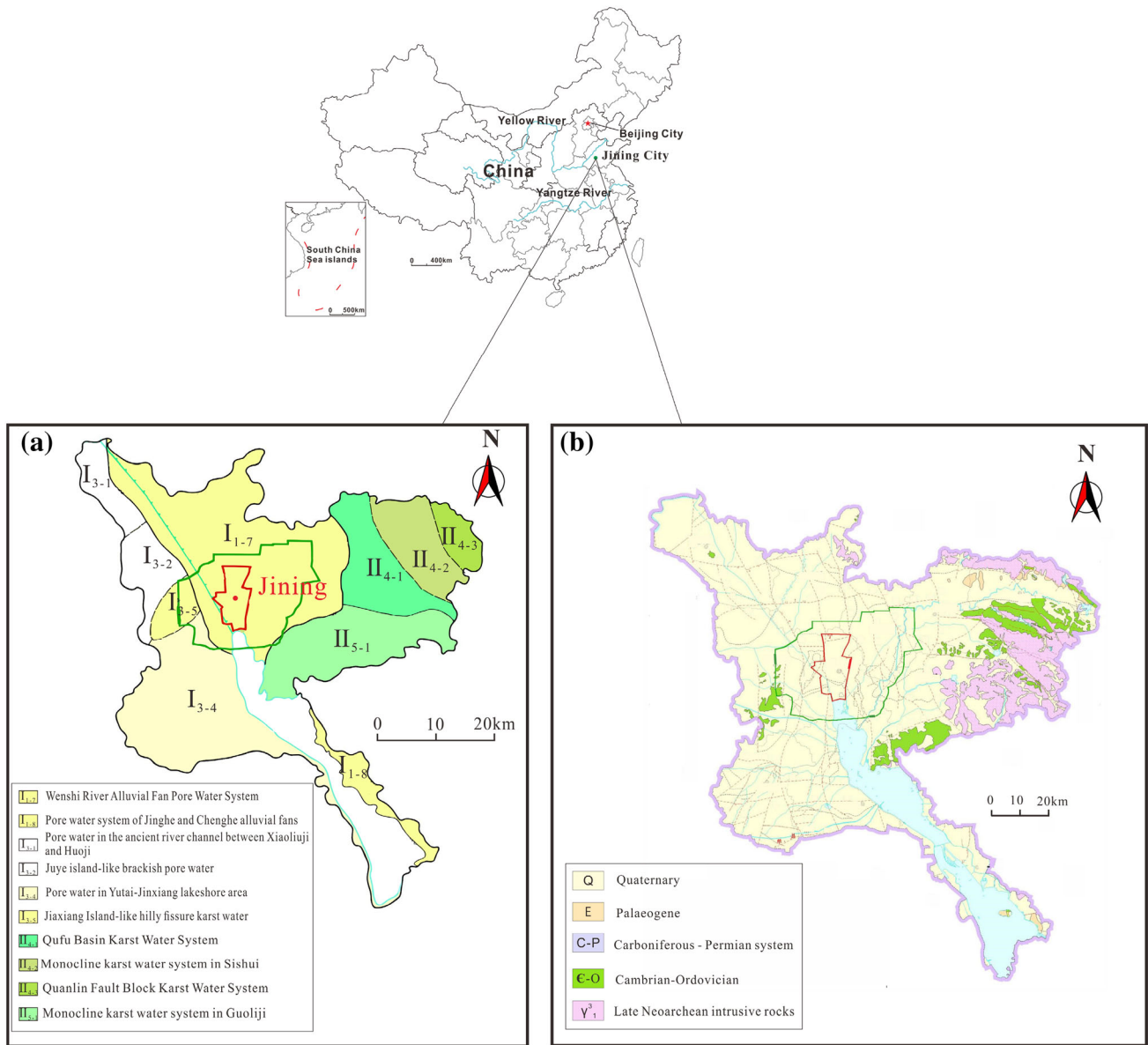


Fig.1 Hydrological and geological map of Jining city (a hydrogeological subdivision map; b geological map)

diving—micro-pressurized water and deep pore pressurized water.

3 Numerical models and theoretical foundations

3.1 Biot consolidation settlement theory

Soil consolidation occurs when the water inside a soil body slowly seeps out under load and gradually decreases in volume. This consolidation phenomenon causes the soil to compress and deform and causes the strength of the soil to grow gradually. In 1941, Biot derived a three-dimensional

consolidation equation reflecting the interrelationship between pore pressure dissipation and soil skeleton deformation[22]. This equation lays the theoretical foundation of flow-solid coupling in porous media.

In the coupled model of groundwater flow and porous media, Biot derived a three-dimensional consolidation equation for the mean total stress of the soil with time by considering the mutual coupling relationship between pore water pressure dissipation and skeletal deformation during water loss consolidation soil. The stress–strain principal structure relationship can be expressed as a tensor.

$$\sigma = C : \varepsilon - \alpha_B p_f I \tag{1}$$

where σ is the stress tensor; ε is the strain tensor. The symbol “:” indicates the second-order tensor product. α_B is the Biot-Willis coefficient; p_f is fluid pore pressure. C is the fourth-order elastic tensor obtained by measuring the stress–strain variation relationship in a soil body under constant pore water pressure. I is the unit matrix.

The equilibrium equation of porous media material under self-weight load is:

$$-\nabla \cdot \sigma = \rho_{av}g = (\rho_f \varepsilon_p + \rho_d)g \tag{2}$$

where ρ_{av} , ρ_f , ρ_d represent the average density, fluid density, and dry density, respectively. ε_p is the porosity, g is the gravitational acceleration.

The geometric equation for the deformation of porous media materials is:

$$\varepsilon = \frac{1}{2} [\nabla u + (\nabla u)^T] \tag{3}$$

where u is displacement tensor.

The flow field equations in the porous medium model can be established by combining Darcy’s law and the fluid mass conservation equation for fluid motion.

$$\rho_f S \frac{\partial p_f}{\partial t} + \nabla \cdot \rho_f \left[-\frac{k}{\mu} (\nabla p_f + \rho_f g \nabla D) \right] = -\rho_f \alpha_B \frac{\partial}{\partial t} \varepsilon_{vol} \tag{4}$$

$$S = \frac{\varepsilon_p}{K_f} + (\alpha_B - \varepsilon_p) \frac{1 - \alpha_B}{K_d} \tag{5}$$

where ε_{vol}/t is the volumetric strain rate of the porous matrix. The storage term S is calculated by Eq. 5. The term to the right of the equal sign can be interpreted as the expansion rate of the pore space. k is the permeability; μ is the dynamic viscosity; D is the water head; K_f is the hydraulic conductivity of fluid; K_d is the hydraulic conductivity of dry.

3.2 Numerical calculation model

This paper uses COMSOL software to simulate land subsidence caused by groundwater mining. The stratum of the study area is the Quaternary loose topsoil layer, depth $0 \sim -200$ m. The model generalizes the topsoil layer into

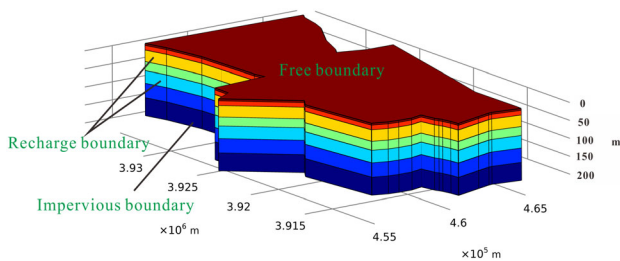


Fig. 2 Numerical model

seven layers (Fig. 2), and the stratigraphic parameters are shown in Table 1.

The Jining study area has 125 water source pumping wells, mainly concentrated in Suzhuang, Shaokanghu, Chengbei, Fenghuangtai, and Chengnan. Water source pumping wells have the characteristics of high pumping flow and concentration of pumping wells. Pumping flows include $2400 \text{ m}^3/\text{d}$, $2880 \text{ m}^3/\text{d}$, $3000 \text{ m}^3/\text{d}$, and $1500 \text{ m}^3/\text{d}$. In addition, there are a large number of self-contained urban wells, rural single centralized water supply source wells, and agricultural irrigation water. These wells are widely distributed, with scattered pumping wells and small pumping flows. Based on the measured pumping information and the extraction well information sheet, the location of the well sites and the extraction volume of each extraction well are obtained (Fig. 3). The pumping level is the second compression layer group.

3.3 Model feasibility analysis

The model modeled the actual pumping wells according to the geological and hydrological data statistics. The initial state of land subsidence in Jining in 1990 is used as the initial state, and the extraction is calculated according to the actual amount of water pumped. Numerical simulation can realistically simulate the land subsidence caused by groundwater mining in Jining.

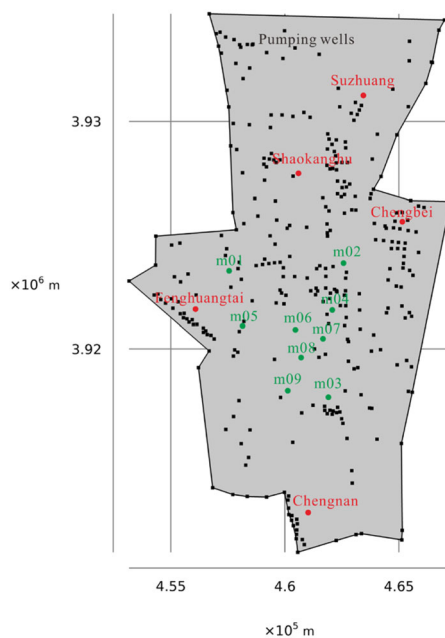
The land subsidence at nine measurement points from 1991 to 1998 was selected as a validation object to verify the accuracy of the numerical calculation model. The locations of the monitoring points are shown in Fig. 3. The model calculation results were compared and analyzed with their actual measured values (Fig. 4). Due to the limited measured data, the selected monitoring points are mainly located in the middle of the model. The difference between the calculated and monitored results at point m04 is the largest, with a difference of 6.3 mm. There are six monitoring points with a difference of 5 mm or less. The point with the largest error value is point m03, with an error value of 7.5%. Seven points have an error of less than 5%.

Here is a comprehensive analysis of the reasons for errors in the monitoring points. In the 3D numerical calculation process, land subsidence is caused entirely by groundwater extraction without considering other factors. Numerous influencing factors exist in practice, and measurement errors cannot be excluded. The calculated subsidence trend and the amount of subsidence agreed with the actual measured values considering errors. The margin of error is within 7.5%.

The establishment of the numerical model and the error analysis of the numerical results are analyzed. It has been proved that the numerical model can better reproduce the

Table 1 Table of stratigraphic parameters

Stratigraphic	Thickness m	Young's modulus MPa	Poisson's ratio	Density kg/m ³	Porosity	Permeability coefficient m/s
Topsoil layer	5	120	0.3	1950	0.47	1e-6
The first compression	13	60	0.3	2000	0.45	1e-10
Layer group						
The first aquifer group	32	150	0.35	2100	0.4	6e-5
The second compression	25	65	0.3	2030	0.45	1e-10
Layer group						
The second aquifer group	35	180	0.35	2150	0.4	1e-5
Semi-cemented layer	40	200	0.35	2150	0.4	1e-5
Clay layer	50	60	0.2	2100	0.45	1e-10

**Fig. 3** Distribution of pumping wells

historical process of subsidence caused by groundwater extraction in the study area of Jining. And the model can be used to predict land subsidence.

4 Results and discussion

4.1 Land subsidence development trend

COMSOL Multiphysics is a mathematical approach to solving real-world physical phenomena by solving partial differential equations or systems of partial differential equations for the simulation of real physical phenomena based on the finite element method. In this paper, a fluid–solid coupling model is constructed based on COMSOL

software. The model includes 57,487 domain cells, 20,431 boundary cells and 3194 edge cells. The model is solved using parallel computation of sparse linear systems.

Based on this model, calculations were performed to simulate the historical process of land subsidence induced by groundwater mining in the study area of Jining. Figure 5 shows the land subsidence cloud map in the study area. In the early days of the study, pumping wells in Jining were mainly concentrated in urban areas, primarily urban self-provided wells. In 2000, land subsidence areas were mainly concentrated in urban locations, away from the five primary water sources (Fig. 6). The maximum urban land subsidence is 154.5 mm. The largest land subsidence among the five primary water sources is about 60 mm at the Chengbei water source. As the city grows, urban water consumption increases. Jining has added water sources in the Chengbei, Chengnan, Shaokanghu, and Suzhuang. In 2010, the maximum urban land subsidence was 195.5 mm. The land subsidence of the Chengbei water source has increased significantly, with land subsidence of about 120 mm. The laying of water wells in urban areas has substantially increased urban land subsidence. To ensure urban water and reduce ground subsidence, Jining has increased water wells in three primary water sources: Fenghuangtai, Shaokanghu, and Suzhuang, far from urban areas. In 2020, the maximum land subsidence in the study area was 217.4 mm. Shaokanghu and Suzhuang water sources experienced significant land subsidence. Compared to 2010, land subsidence increased significantly, with a maximum value of about 180 mm.

The land subsidence caused by groundwater extraction is positively correlated with the time and amount of pumping. The location with high pumping capacity and long pumping time produces significant land subsidence. In 1990, many self-provided wells were used in the city of Jining. Groundwater extraction over a long period has resulted in widespread land subsidence in the city of Jining.

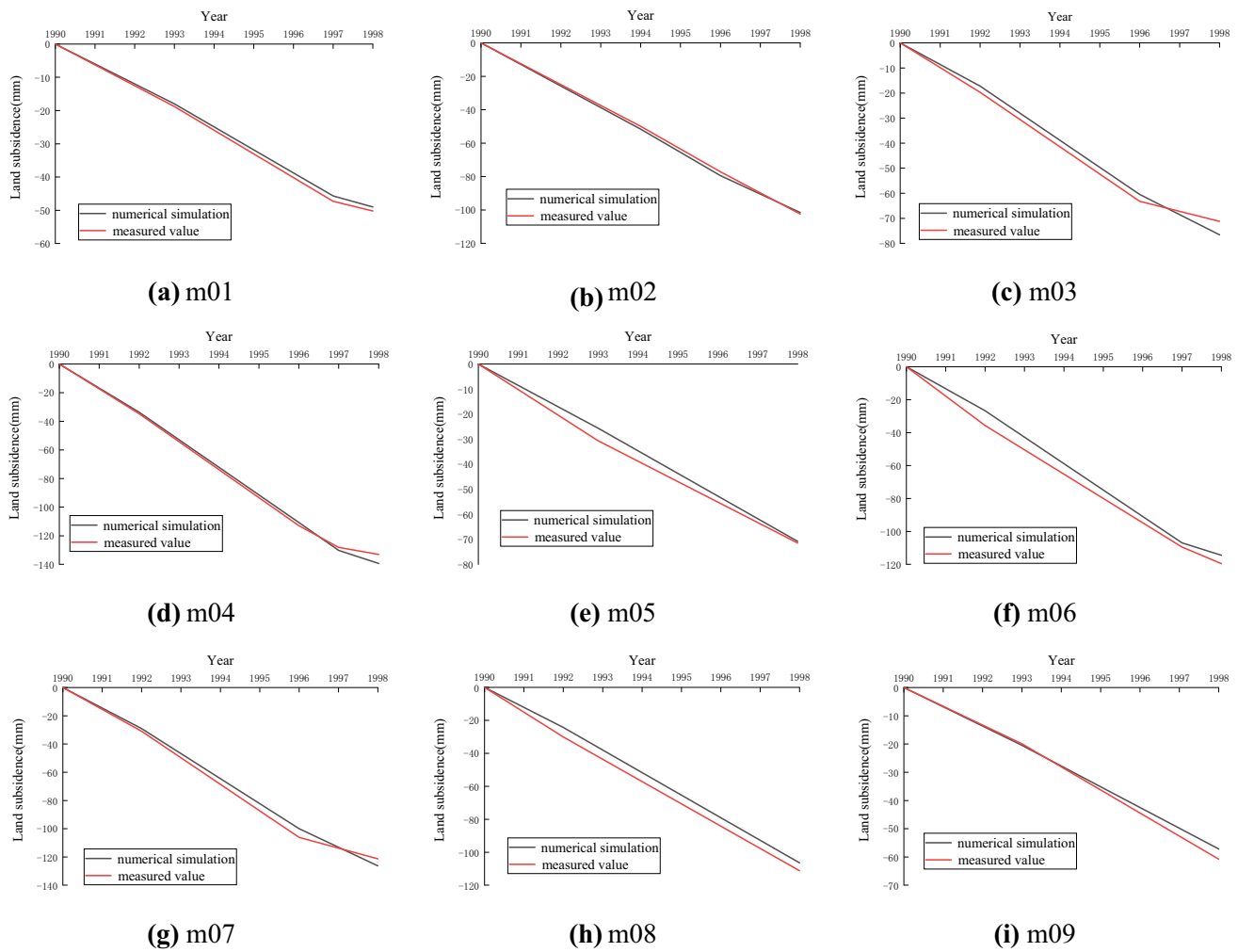


Fig. 4 Comparison of actual and simulated monitoring points

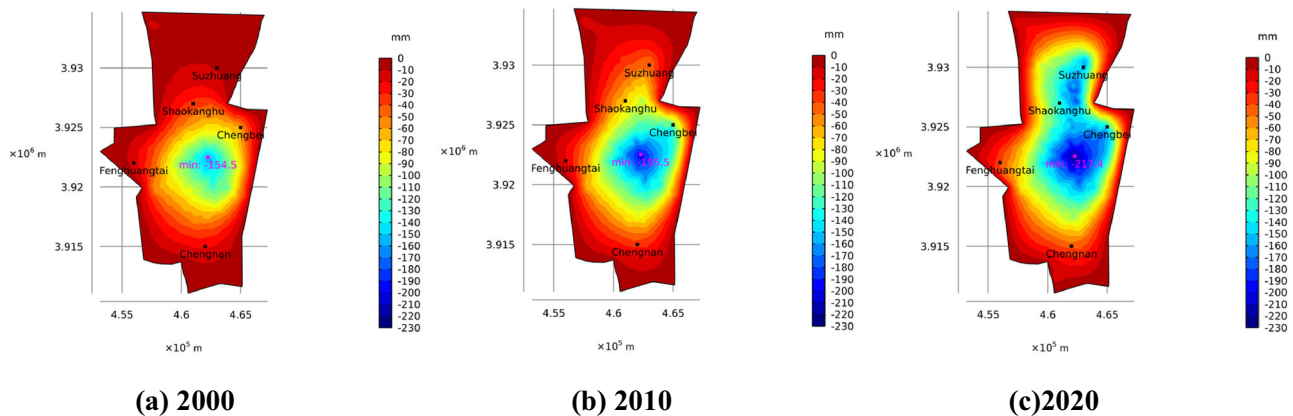


Fig. 5 Land subsidence development

Land subsidence is influenced by the amount of water pumped per unit time. After 2008, many additional water wells were installed in the Suzhuang and Shaokanghu areas. The two primary water sources with large numbers

and density of pumping wells have significantly increased the amount of water pumped. In 2020, the area experienced severe land subsidence with a maximum of about 180 mm. Therefore, it is necessary to lay pumping wells reasonably,

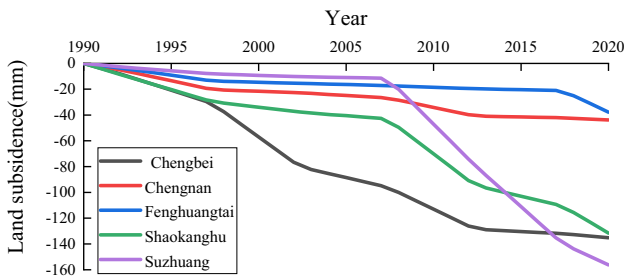


Fig. 6 Land subsidence curves of five water sources

control the amount of water pumped from a single well, and reduce the density of pumping well distribution. These methods can effectively reduce land subsidence and lower the peak land subsidence within acceptable limits.

4.2 Land subsidence prediction

The numerical calculation is carried out to predict the land subsidence change rule in the study area in 2030 by keeping the pumping amount unchanged (Fig. 7). The land subsidence in the study area gradually increases with time. In 2030, the maximum land subsidence will be 224 mm (Fig. 7b). From 2020 to 2030, there will be less change in land subsidence in urban areas of Jining. The land subsidence rate gradually decreases. The maximum land subsidence increased by 7 mm in ten years. The land subsidence of the Shaokanghu and Suzhuang water sources is further developed, with a maximum of 210 mm.

Before 2030, the land subsidence in Shaokanghu, Suzhuang, and Fenghuangtai water sources is still developing. The land subsidence is stable in the Chengbei and

Chengnan water sources and urban locations. The land subsidence rate gradually decreases, and the stratum gradually stabilizes after a long period of groundwater extraction. The new additional pumping wells will cause further land subsidence development and increase the subsidence rate. And this will create new subsidence centers in the vicinity of the pumping wells. Therefore, appropriate deployment of pumping wells can effectively control land subsidence and ensure urban water use. The land subsidence center can be artificially interfered with by changing the area where the pumping wells are deployed.

4.3 Prediction of land subsidence under different pumping conditions

The amount of mining at the water source was modified to verify the effect of different mining on land subsidence. The change in pumping volume is timed to 2020. The pumping wells modified in this paper are fourteen wells at the Suzhuang water source, nineteen wells at the Fenghuangtai water source, and twenty wells at the Shaokanghu water source. This paper calculates two working conditions: a 30% increase and a 30% decrease in mining volume.

Keeping the amount of water pumped constant (Fig. 8a), the center of land subsidence in Jining will gradually develop towards the north and west of the study area in the coming years due to additional wells. The study area will form the Shaokang Lake, Suzhuang subsidence center, and Fenghuangtai subsidence center. The maximum subsidence is 35 mm in Suzhuang and Shaokanghu during the ten years. The maximum subsidence in the Fenghuangtai area is about 20 mm.

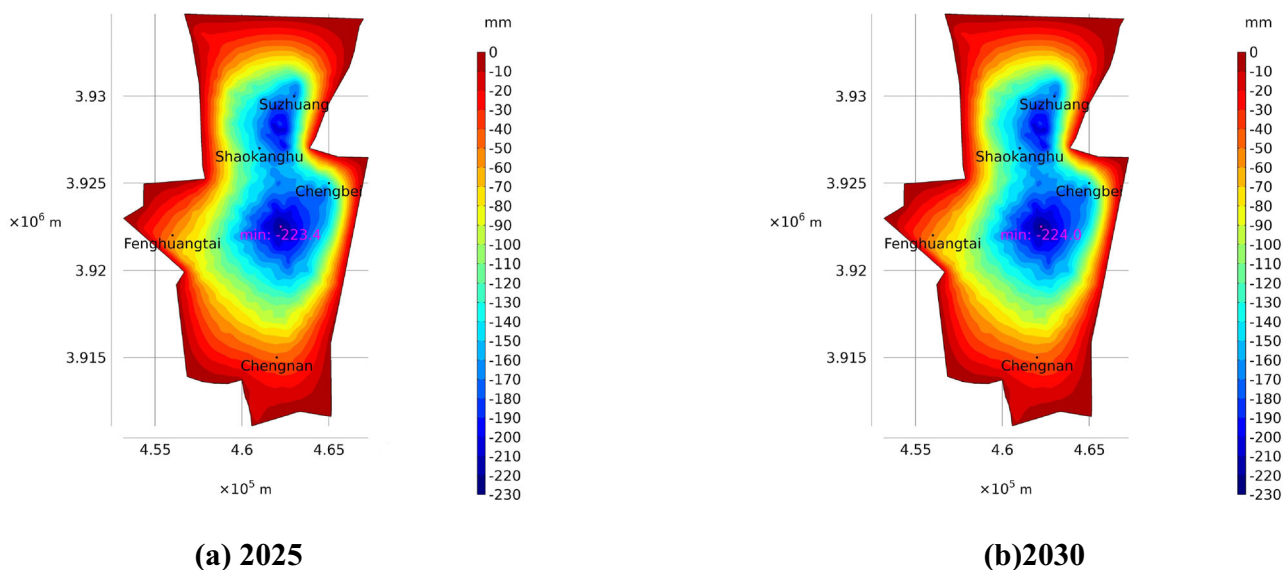


Fig. 7 Cloud map of land subsidence prediction

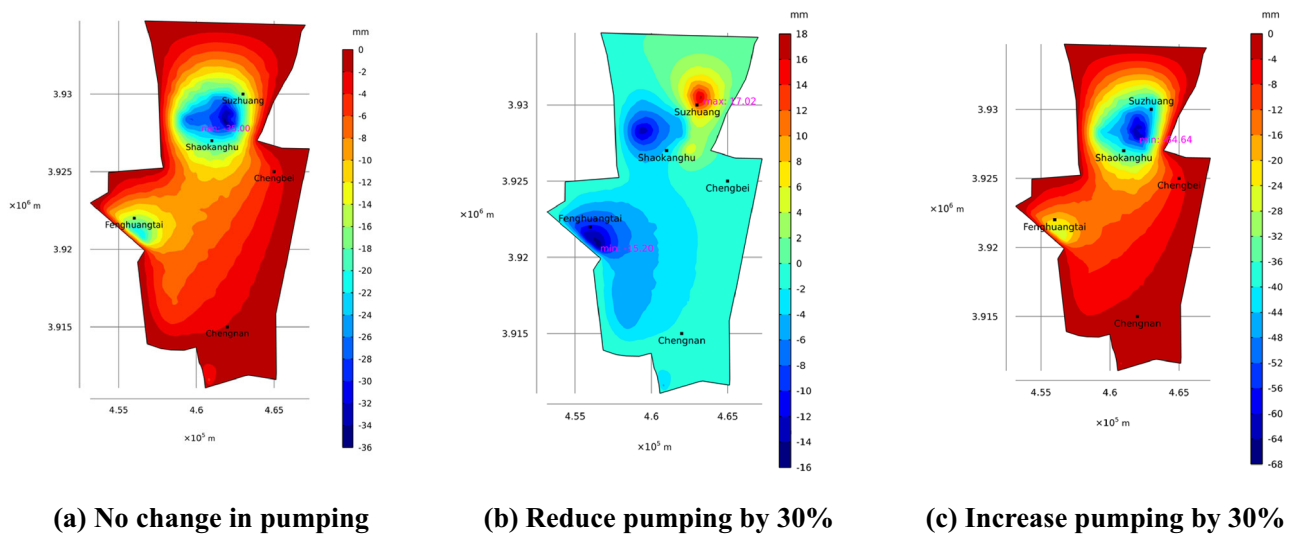


Fig. 8 Cloud map of land subsidence from 2020 to 2030

When groundwater extraction is reduced by 30%, there is a significant change in the land subsidence pattern in the study area (Fig. 8b). When pumping decreases, the land subsidence decreases accordingly. In 2020–2030, the maximum land subsidence value is 15.2 mm, located at the water source of Fenghuangtai. The ground rebounded at the Suzhuang water source. In 2030, the study area will form two types of centers: the Fenghuangtai-Shaokanghu land subsidence center and the Suzhuang land resilience center. The land subsidence patterns of the three primary water sources are different, related to the pumping time of the pumping wells. The Suzhuang water source began pumping water mainly in 2014. Keeping the pumping volume constant, the rate of land subsidence gradually decreases with time. When pumping is significantly reduced, the land surface will rebound due to groundwater recharge of the aquifer. The water source of Fenghuangtai and Shaokanghu started pumping water mainly in 2019 and 2020. The land subsidence decreases due to reduced pumping.

When the pumping volume is increased by 30%, the land subsidence pattern is unchanged (Fig. 8c). And the value of land subsidence increases significantly. In 2020–2030, the maximum value of the land subsidence is 64.6 mm, located near the water source of Suzhuang and Shaokanghu. The land subsidence increased by nearly 30 mm compared to under regular pumping. The land subsidence at the Fenghuangtai water source also increased relatively, with land subsidence of about 30 mm.

The amount of water pumped is one of the main factors influencing land subsidence. When groundwater extraction increases, the land subsidence increases accordingly. Under the premise of ensuring urban water use, appropriate reduction of pumping can effectively reduce land subsidence. With the groundwater recharge of the aquifer, the

ground will rebound, which can effectively alleviate the land subsidence problem.

5 Conclusion

This paper establishes a flow-solid coupling model by COMSOL software and analyzes the land subsidence law caused by water pumping in Jining. And the article predicts the change of land subsidence pattern by 2030. The following conclusions were obtained.

- (1) Land subsidence caused by groundwater extraction positively correlates with pumping time and the amount of water pumped. Prolonged and high flow pumping will result in significant land subsidence.
- (2) This paper predicts the land subsidence pattern in the study area of Jining by 2030. Before 2030, the land subsidence is still in development in Shaokanghu, Suzhuang, and Fenghuangtai water sources. The land subsidence is stable at the location of Chengbei, Chengnan water sources, and the urban area.
- (3) The article predicts the land subsidence pattern with different pumping amounts. Under the condition of reducing 30% of pumping water, the study area forms the land subsidence center of Fenghuangtai-Shaokanghu and the ground rebound center of Suzhuang. Under the condition of increasing 30% of pumping water, the study area forms the Shaokanghu-Suzhuang subsidence center and the Fenghuangtai subsidence center.

Acknowledgements Research in this paper is supported by the National Natural Science Foundation of China (Grant Numbers 41877239, 51379112, 51422904, 40902084, and 41772298),

Fundamental Research Fund of Shandong University (Grant Number 2018JC044), and the Natural Science Foundation of Shandong Province (Grant Numbers JQ201513 and 2019GSF111028).

Author contributions HC: software, theory, writing—original draft preparation, reviewing, visualization. YX: conceptualization, methodology, writing—original draft preparation, funding acquisition. DQ: reviewing, editing.

Data availability The datasets generated during and/or analysed during the current study are not publicly available due to urban land subsidence data confidentiality. Still, they are available from the corresponding author on reasonable request.

Declarations

Competing interests The authors declare that they have no known competing financial interests or personal relationships that could have appeared to influence the work reported in this paper.

References

- Rahmati, O., Golkarian, A., Biggs, T., Keesstra, S., Mohammadi, F., Daliakopoulos, I.N.: Land subsidence hazard modeling: machine learning to identify predictors and the role of human activities. *J. Environ. Manag.* **236**, 466–480 (2019)
- Castellazzi, P., Garfias, J., Martel, R., Brouard, C., Rivera, A.: InSAR to support sustainable urbanization over compacting aquifers: the case of Toluca Valley, Mexico. *Int. J. Appl. Earth Observ. Geoinf.* **63**, 33–44 (2017)
- Ding, P., Jia, C., Di, S., Wang, L., Bian, C., Yang, X.: Analysis and prediction of land subsidence along significant linear engineering. *Bull. Eng. Geol. Environ.* **79**(10), 5125–5139 (2020)
- Morton, R.A., Bernier, J.C., Barras, J.A.: Evidence of regional subsidence and associated interior wetland loss induced by hydrocarbon production, Gulf Coast region, USA. *Environ. Geol.* **50**(2), 261–274 (2006)
- Bell, F.G., Stacey, T.R., Genske, D.D.: Mining subsidence and its effect on the environment; some differing examples. *Environ. Geol. (Berlin)* **40**(1–2), 135–152 (2000)
- Jia, C., Zhang, Y., Han, J., Xu, X.: Susceptibility area regionalization of land subsidence based on extenics theory. *Clust. Comput.* **20**, 53–66 (2017)
- Herrera-García, G., Ezquerro, P., Tomás, R., Béjar-Pizarro, M., López-Vinielles, J., Rossi, M., et al.: Mapping the global threat of land subsidence. *Science (American Association for the Advancement of Science)* **371**(6524), 34–36 (2021)
- Conway, B.D.: Land subsidence and earth fissures in south-central and southern Arizona, USA. *Hydrogeol. J.* **24**(3), 649–655 (2016)
- Chaussard, E., Wdowinski, S., Cabral-Cano, E., Amelung, F.: Land subsidence in central Mexico detected by ALOS InSAR time-series. *Remote Sens. Environ.* **140**, 94–106 (2014)
- Abidin, H.Z., Gumilar, I., Andreas, H., Murdohardono, D., Fukuda, Y.: On causes and impacts of land subsidence in Bandung Basin, Indonesia. *Environ. Earth Sci.* **68**(6), 1545–1553 (2013)
- Phien-Wej, N., Giao, P.H., Nutalaya, P.: Land subsidence in Bangkok, Thailand. *Eng. Geol.* **82**(4), 187–201 (2006)
- Gong, X., Geng, J., Sun, Q., Gu, C., Zhang, W.: Experimental study on pumping-induced land subsidence and earth fissures: a case study in the Su-Xi-Chang region, China. *Bull. Eng. Geol. Environ.* **79**(9), 4515–4525 (2020)
- Shen, S., Xu, Y.: Numerical evaluation of land subsidence induced by groundwater pumping in Shanghai. *Can. Geotech. J.* **48**(9), 1378–1392 (2011)
- Qin, H., Andrews, C.B., Tian, F., Cao, G., Luo, Y., Liu, J., et al.: Groundwater-pumping optimization for land-subsidence control in Beijing plain, China. *Hydrogeol. J.* **26**(4), 1061–1081 (2018)
- Guo, J., Hu, J., Li, B., Zhou, L., Wang, W.: Land subsidence in Tianjin for 2015 to 2016 revealed by the analysis of Sentinel-1A with SBAS-InSAR. *J. Appl. Remote Sens.* **11**(2), 26024 (2017)
- Wang, Y., Wang, Z., Cheng, W.: A review on land subsidence caused by groundwater withdrawal in Xi’an, China. *Bull. Eng. Geol. Env.* **78**(4), 2851–2863 (2019)
- Ma, R., Wang, Y., Ma, T., Sun, Z., Yan, S.: The effect of stratigraphic heterogeneity on areal distribution of land subsidence at Taiyuan, northern China. *Environ. Geol.* **50**(4), 551–568 (2006)
- Figueroa-Miranda, S., Tuxpan-Vargas, J., Alfredo Ramos-Leal, J., Manuel Hernandez-Madrigal, V., Irene Villasenor-Reyes, C.: Land subsidence by groundwater over-exploitation from aquifers in tectonic valleys of Central Mexico: a review. *Eng. Geol.* **246**, 91–106 (2018)
- Galloway, D.L., Burbey, T.J.: Review: regional land subsidence accompanying groundwater extraction. *Hydrogeol. J.* **19**(8), 1459–1486 (2011)
- Xu, Y., Shen, S., Cai, Z., Zhou, G.: The state of land subsidence and prediction approaches due to groundwater withdrawal in China. *Nat. Hazards* **45**(1), 123–135 (2008)
- Li, J.: Transient radial movement of a confined leaky aquifer due to variable well flow rates. *J. Hydrol.* **333**(2–4), 542–553 (2007)
- Biot, M.A.: General theory of three-dimensional consolidation. *J. Appl. Phys.* **12**(2), 155–164 (1941)
- Mahmoudpour, M., Khamehchiyan, M., Nikudel, M.R., Ghassemi, M.R.: Numerical simulation and prediction of regional land subsidence caused by groundwater exploitation in the southwest plain of Tehran, Iran. *Eng. Geol.* **201**, 6–28 (2016)
- Jafari, F., Javadi, S., Golmohammadi, G., Karimi, N., Mohammadi, K.: Numerical simulation of groundwater flow and aquifer-system compaction using simulation and InSAR technique: Saveh basin, Iran. *Environ. Earth Sci.* **75**(9), 1–10 (2016)
- Guzy, A., Malinowska, A.: State of the art and recent advancements in the modelling of land subsidence induced by groundwater withdrawal. *Water* **12**(7), 2051 (2020)
- Qu, F., Lu, Z., Zhang, Q., Bawden, G.W., Kim, J., Zhao, C., et al.: Mapping ground deformation over Houston-Galveston, Texas using multi-temporal InSAR. *Remote Sens. Environ.* **169**, 290–306 (2015)
- Lo W., Purnomo S. N., Dewanto B. G., Sarah D., Sumiyanto: Integration of numerical models and InSAR techniques to assess land subsidence due to excessive groundwater abstraction in the coastal and lowland regions of Semarang City. *Water (Basel)* **14**(2), 201 (2022)
- Bajni, G., Apuani, T., Beretta, G.P.: Hydro-geotechnical modelling of subsidence in the Como urban area. *Eng. Geol.* **257**, 105144 (2019)
- Sayyaf, M., Mahdavi, M., Barani, O.R., Feiznia, S., Motamedvaziri, B.: Simulation of land subsidence using finite element method: Rafsanjan plain case study. *Nat. Hazards* **72**(2), 309–322 (2014)
- Cui, Y., Su, C., Shao, J., Wang, Y., Cao, X.: Development and application of a regional land subsidence model for the plain of Tianjin. *J. Earth Sci.* **25**(3), 550–562 (2014)
- Shi, X., Wu, J., Ye, S., Zhang, Y., Xue, Y., Wei, Z., et al.: Regional land subsidence simulation in Su-Xi-Chang area and Shanghai City, China. *Eng. Geol.* **100**(1–2), 27–42 (2008)
- Hu, B., Zhou, J., Xu, S., Chen, Z., Wang, J., Wang, D., et al.: Assessment of hazards and economic losses induced by land

subsidence in Tianjin Binhai new area from 2011 to 2020 based on scenario analysis. *Nat. Hazards* **66**(2), 873–886 (2013)

33. Gao, P.H., Phien-Wej, N., Honjo, Y.: FEM quasi-3D modelling of responses to artificial recharge in the Bangkok multiaquifer system. *Environ. Model. Softw.* **14**(2–3), 141–151 (1999)
34. Larson, K., Basagaoglu, H., Marino, M.: Prediction of optimal safe ground water yield and land subsidence in the Los Banos-Kettleman City area, California, using a calibrated numerical simulation model. *J. Hydrol.* **242**(1–2), 79–102 (2001)

Publisher's Note Springer Nature remains neutral with regard to jurisdictional claims in published maps and institutional affiliations.

Springer Nature or its licensor holds exclusive rights to this article under a publishing agreement with the author(s) or other rightsholder(s); author self-archiving of the accepted manuscript version of this article is solely governed by the terms of such publishing agreement and applicable law.



Hong Chen received a B.S. degree in mining engineering from Northeastern University, Shenyang, China, in 2020. He is currently studying for a master's degree in geotechnical engineering at Shandong University, China. His research interests are land subsidence.



Yiguo Xue Ph.D., Professor of the China University of Geosciences, Beijing. Mainly engaged in the field of advanced geological forecasting and geological engineering investigation.



Daohong Qiu Ph.D., Professor of Shandong University. Mainly engaged in advanced geological forecasting and TBM tunneling performance prediction.